Electronic Supplementary Material (ESI) for Dalton Transactions.

Potassium Uranyl Borate 3D Framework Compound Resulted from Temperature Directed Hydroborate Condensation: Structure, Spectroscopy, and Dissolution Studies

Xiaomei Xu [a]† Zhiyong Liu [a]†, Shitong Yang [a], Lanhua Chen [a], Juan Diwu [a], Evgeny V. Alekseev [b], Zhifang Chai [a], Thomas E. Albrecht-Schmitt [c], Shuao Wang [a*]

[a.] School for Radiological and Interdisciplinary Sciences (RAD-X) and Collaborative Innovation Center of Radiation Medicine of Jiangsu Higher Education Institutions, Jiangsu 215123, China. Email: shuaowang@suda.edu.cn

[b.] Institute of Energy and Climate Research (IEK-6), Forschungszentrum Jülich GmbH, 52428 Jülich, Germany.

[c.] Department of Chemistry and Biochemistry, Florida State University, 95 Chieftain Way, Tallahassee, Florida 32306, USA.

Contents

S1. The picture of potassium uranium borates.

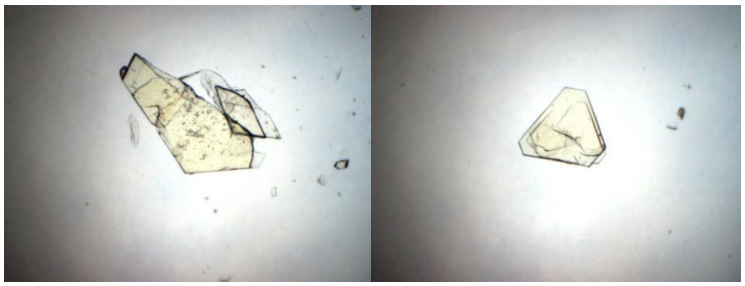

Figure S1. The picture of **KUBO-1** (left) and **KUBO-4** (right) taken under the microscope

S2. The bond distances (Å) for KUBO-4.

Table S1. The bond distances (Å) of UO_8-polyhedron in $K[(UO_2)B_6O_{10}(OH)]\cdot H_2O$ (**KUBO-4**).

Bond	Distance(Å)	Bond	Distance(Å)
U1-O1	1.768(7)	U1-O5	2.564(11)
U1-O2	1.770(8)	U1-O6	2.419(11)
U1-O3	2.400(10)	U1-O7	2.406(10)
U1-O4	2.526(10)	U1-O8	2.585(11)

S3. Powder X-ray diffraction analysis.

The experimental PXRD patterns of **KUBO-1** and **KUBO-4** match well with the simulated ones, revealing that it is a single phase without any impurity. The experimental PXRD patterns are shown in **Figure S2** and **Figure S3**.

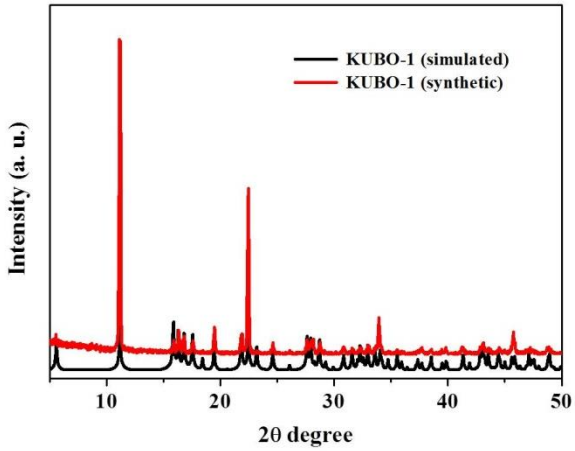

Figure S2. The powder X-ray diffraction (PXRD) patterns of **KUBO-1**

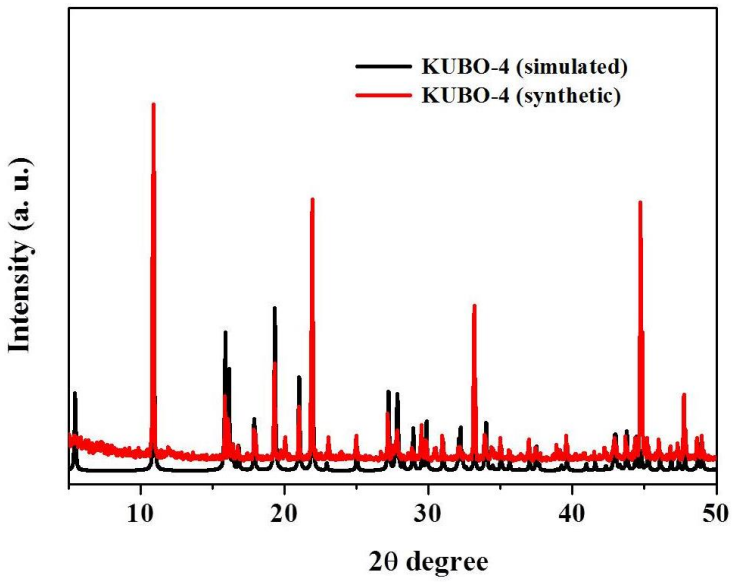

Figure S3. The powder X-ray diffraction (PXRD) patterns of **KUBO-4**

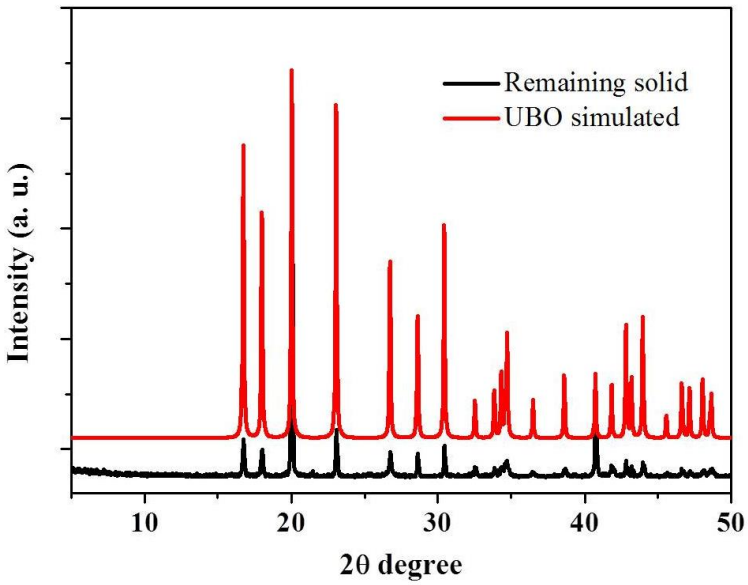

Figure S4. The powder X-ray diffraction (PXRD) patterns of the remaining solids of **KUBO-1** and **KUBO-4** after TG/DSC test

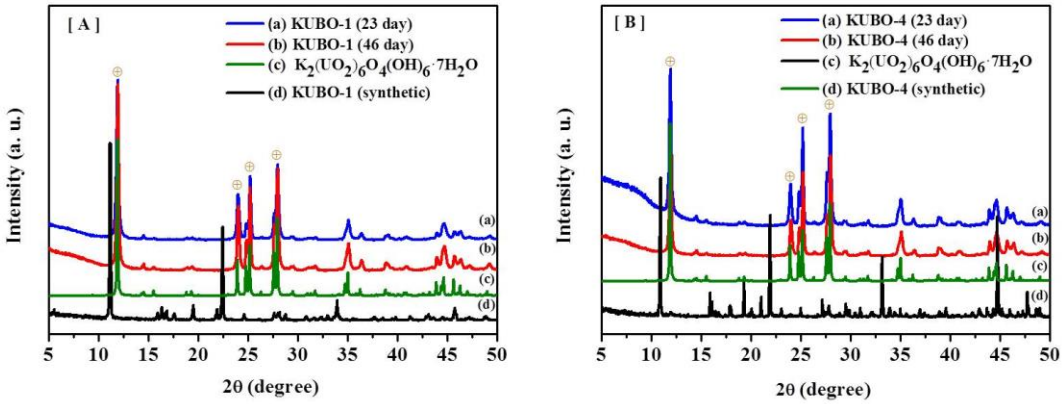

Figure S5. The PXRD patterns of uranyl borates (A, **KUBO-1**; B, **KUBO-4**.) after extraction from background solution of 10 mM $NaNO_3$ at different time intervals (XRD patterns of the remaining solids of uranyl borates phases from solubility experiments during 23 days (a) and 46 days (b), the simulated compreignacite (c), and the initial synthetic uranyl borates (d))

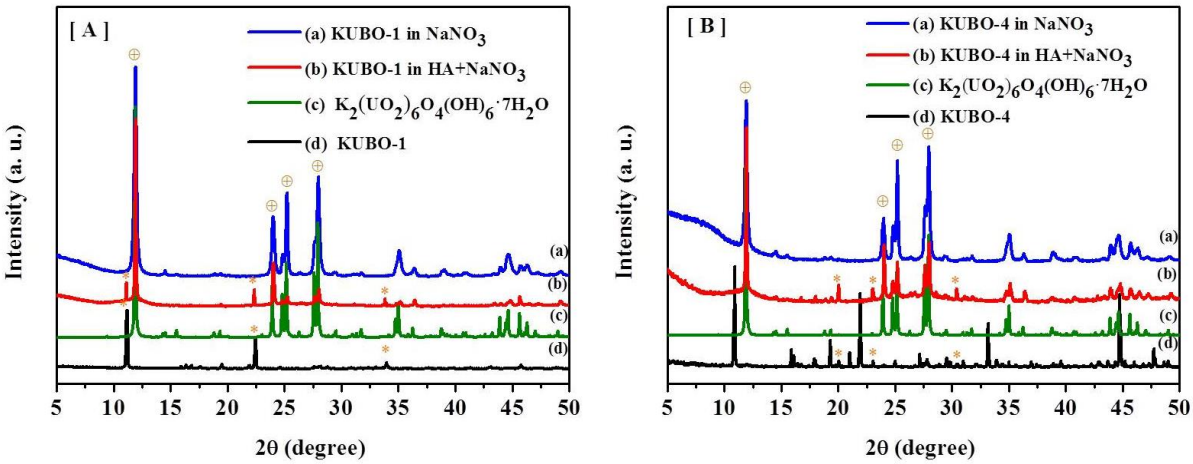

Figure S6. The PXRD patterns of uranyl borates (A, **KUBO-1**; B, **KUBO-4**) after extraction of 23 days in 20 mg (C) /L HA in background solution I = 0.01 M ($NaNO_3$), and only background solution I = 0.01 M ($NaNO_3$) (XRD patterns of the remaining solids of the uranyl borates phases from HA+$NaNO_3$ (a) and only $NaNO_3$ (b) solutions, the simulated compreignacite (c), and the initial synthetic uranyl borates (d))

S4. Dissolution details.

The dissolution experiments with the solid/liquid ratio of 5 mg (U) /20 mL were conducted by suspending ~5 mg (U) of uranium borate solids (~12 mg crystals) to ~20 mL of appropriate nitrate, HA, carbonate, and phosphate solutions in 20 mL head-sealed vials, equilibrating the suspensions for different periods, separating the solids from suspensions, and analyzing the aqueous and solid phases.

In 5 mg (U) /20 mL carbonate system, the dissolution trends were similar for the two uranium borate phases (**Figure S7** A-1, A-2). Eventually the uranium concentration in the solution was about 300 mg/L. The dissolved constant *k* value of **KUBO-1** and **KUBO-4** were 0.0116 h^{-1} and 0.0244 h^{-1} from the Empirical simulations (Eq. (1)), respectively. In the meantime, the dissolution rate of **KUBO-4** was about two times faster than **KUBO-1** in the system of carbonate.

In 5 mg (U)/20 mL HA systems, it took about 249.6 hours and 300 hours to attain pseudo-equilibrium for **KUBO-1** and **KUBO-4** for 22 days experimental test, respectively (**Figure S7** B-1, B-2). After the Empirical simulations (Eq. (1)) fitting, the dissolved constant *k* values were 0.0140 and 0.0111 h^{-1} for **KUBO-1** and **KUBO-4**, respectively.

Table S2. Parameters for simulating the dissolution kinetics of **KUBO-1** and **KUBO-4** in the presence of 5 mg (U)/20 mL and 5 mg (U)/50 mL different ligands systems (**KUBO-1-C**, **KUBO-4-C** for **KUBO-1** and **KUBO-4** with bicarbonate, **KUBO-1-H**, **KUBO-4-H** for **KUBO-1** and **KUBO-4** with humic acids, and **KUBO-1-P**, **KUBO-4-P** for **KUBO-1** and **KUBO-4** with phosphate.).

	KUBO-1-C	**KUBO-4-C**	**KUBO-1-H**	**KUBO-4-H**	**KUBO-1-P**	**KUBO-4-P**
C_{us}(mg/L)/20 mL[a]	290.8	289.9	5.5	5.1	0.096	0.123
C_{us}(mg/L)/50 mL[a]	107.9	116.7	5.5	4.8	0.065	0.065
Fluorescence quantum yield	45.52	5.64	45.52	5.64	45.52	5.64
Specific surface area (m^2/g)	17.138	9.054	17.138	9.054	17.138	9.054
K_1:[k(h^{-1})/20 mL][b]	0.0116	0.0244	0.0140	0.0111	/	/
K_2:[k(h^{-1})/50 mL][b]	0.0320	0.0658	0.0390	0.0301	/	/
Std/50 mL[c]	4.5	3.5	0.36	0.25	0.0050	0.0048
R^2/20 mL	0.9801	0.9929	0.9832	0.9685	/	/
R^2/50 mL	0.9949	0.9849	0.9501	0.9703	/	/
%(U)/20 mL[d]	100	100	1.89	1.71	0.03	0.04
%(U)/50 mL[d]	100	100	5.03	4.11	0.063	0.062

[a] C_{Us}: apparent steady-state concentration of dissolved U in the presence of 5 mg (U)/20 mL and 5 mg (U)/50 mL systems, respectively.

[b] K: dissolution rate constant in the presence of 5 mg (U)/20 mL and 5 mg (U)/50 mL systems, respectively.

[c] Std: standard deviation in the presence of 5 mg (U)/50 mL systems.

[d] %(U): the final dissolved fraction of U in the presence of 5 mg (U)/20 mL and 5 mg (U)/50 mL systems, respectively.

In 5 mg (U) /20 mL phosphate system, the highest aqueous U (VI) concentration was about 0.45 mg/L during 7 hours in the phosphate solution of **KUBO-1**, meanwhile the value for **KUBO-4** sharply increased up to about 0.55 mg/L within 8 hours (**Figure S7** C-1, C-2). Then as a function of time, the aqueous U (VI) concentration slowly decreased. Eventually the pseudo-equilibrium dissolved concentration of U (VI) for **KUBO-1** and **KUBO-4** were 0.096 and 0.123 mg/L, respectively.

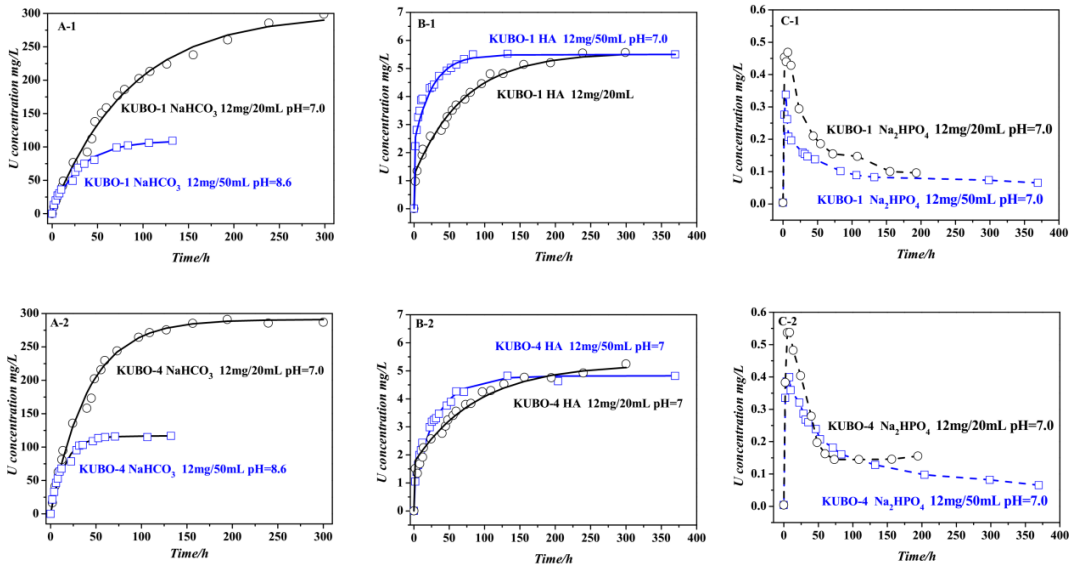

Figure S7. Time evolution of U (aq) concentrations for dissolution experiments using the synthetic **KUBO** crystals: (0.020 g/50 ml and 0.020 g/20 ml) at (A/B/C/D-1) **KUBO-1**, (A/B/C/D-1-2) **KUBO-4**, with different pH (7.03～8.65) in the presence of 10 mM $NaNO_3$, 20 mM $NaHCO_3$, 20 mg (C) /L HA, 20 mM Na_2HPO_4 and I = 0.01 M ($NaNO_3$). Bars represent the standard deviations from duplicate experiments. Solid lines were fitted results from the Eq. (1) for the $NaHCO_3$ and HA

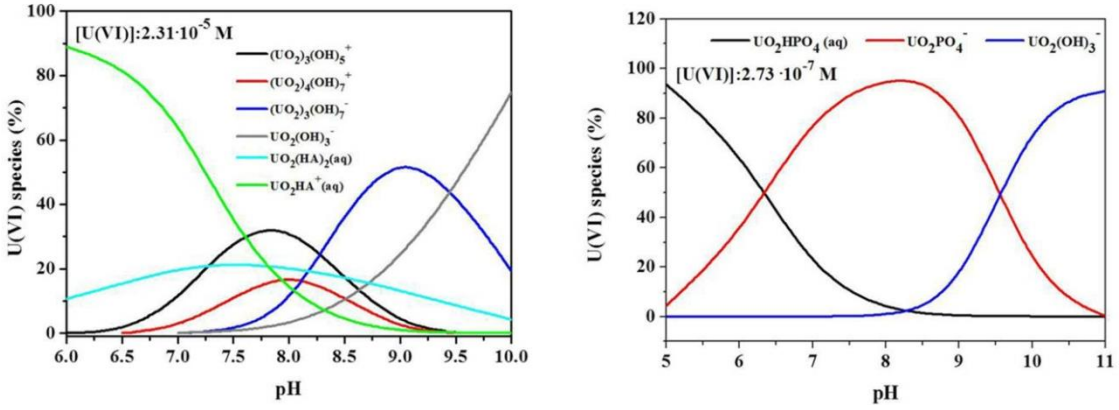

Figure S8. The theoretical main species present in the 0.020 g/50 ml HA and phosphate systems as a function of solution pH based on the experimental concentration conditions. T = 293 K, $NaNO_3$ C = 0.01 mol/L.

S5. Spectroscopic characterizations.

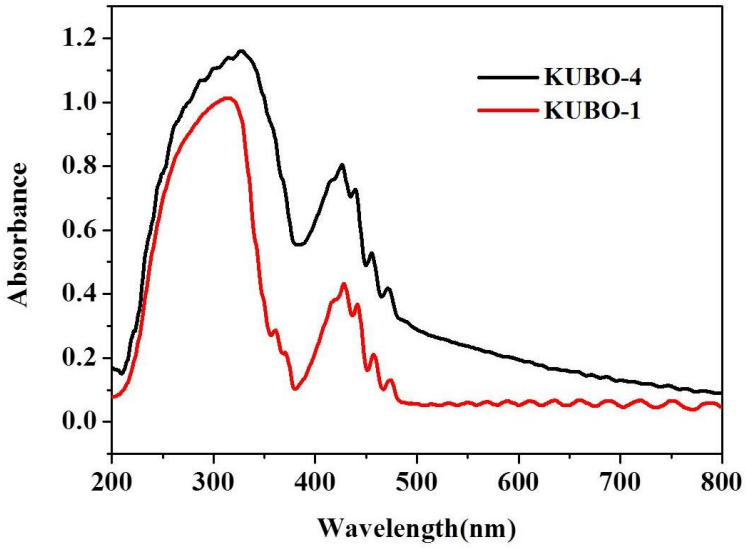

Figure S9. The UV-vis absorption spectra for **KUBO-1** and **KUBO-4** measured at 298 K

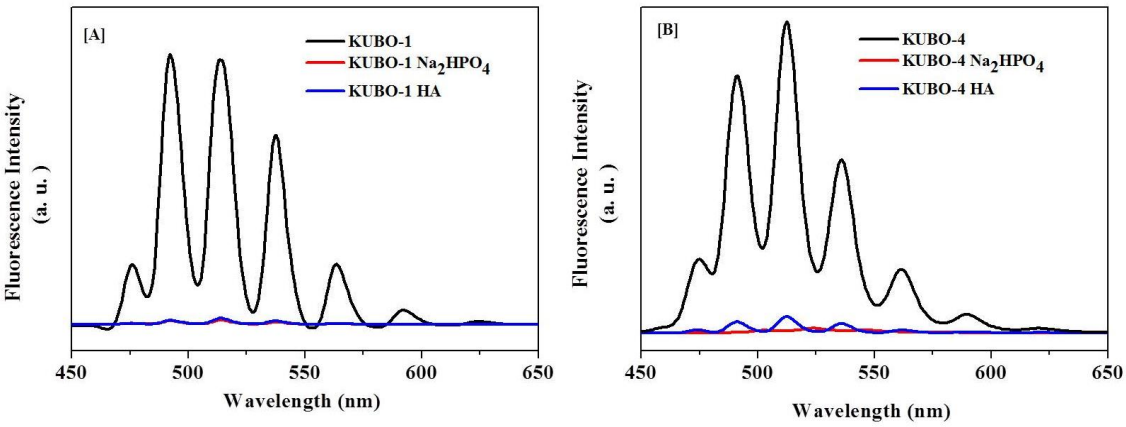

Figure S10. The fluorescence spectra of the original crystals and the residue particles in humic acid and phosphate solutions after 23 days of dissolution (λ_{ex} = 365 nm)

S6. Quantum yield of KUBO-1 and KUBO-4.

The quantum yield of **KUBO-1** and **KUBO-4** were collected by Fluorolog-3 spectrofluorometers showing great difference values (**KUBO-1**: Φ_{QY} = 45.52 % and **KUBO-4**: Φ_{QY} =5.64 %) for **KUBO-1** and **KUBO-4**.

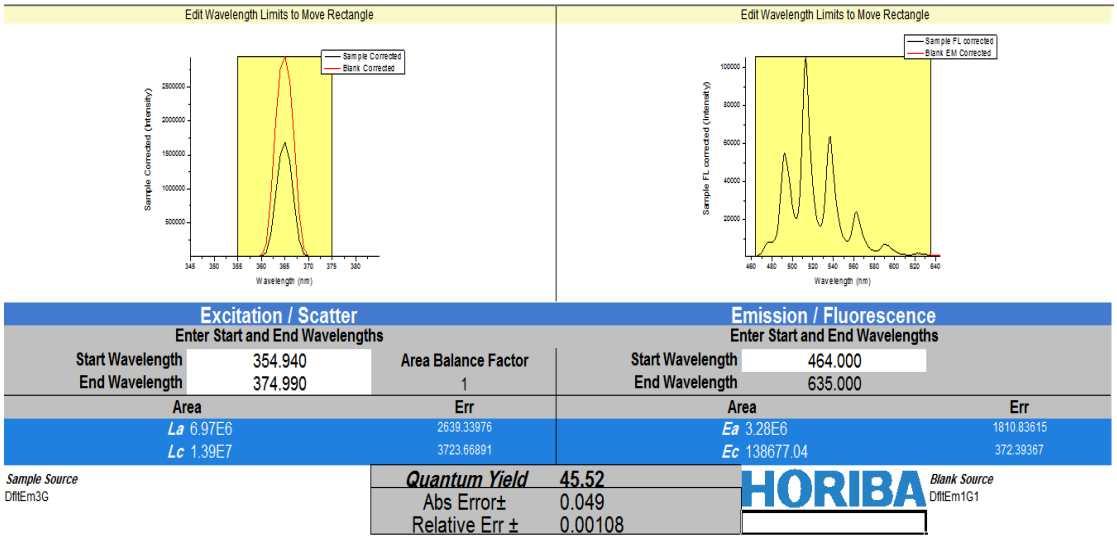

Figure S11. The analysis of quantum yield of **KUBO-1**

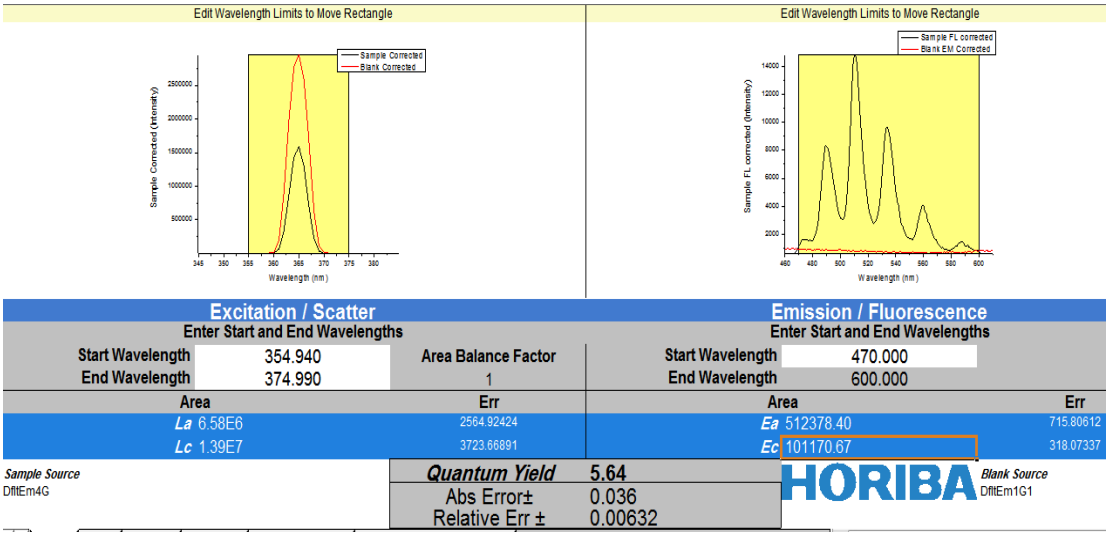

Figure S12. The analysis of quantum yield of **KUBO-4**

S7. Scanning electron microscopy-energy dispersive spectroscopy (SEM-EDS)

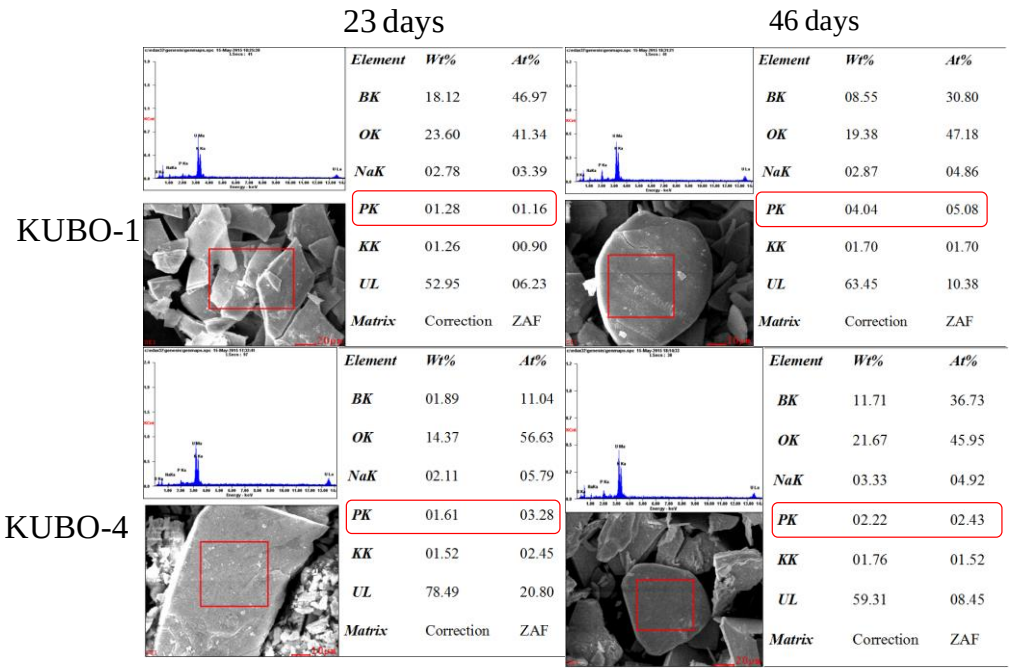

Figure S13. SEM-EDS spectra of the remaining solids of the uranyl borates phases collected from 20 mM Na_2HPO_4 solution with I = 0.01 M ($NaNO_3$), after 23 and 46 days of experiments